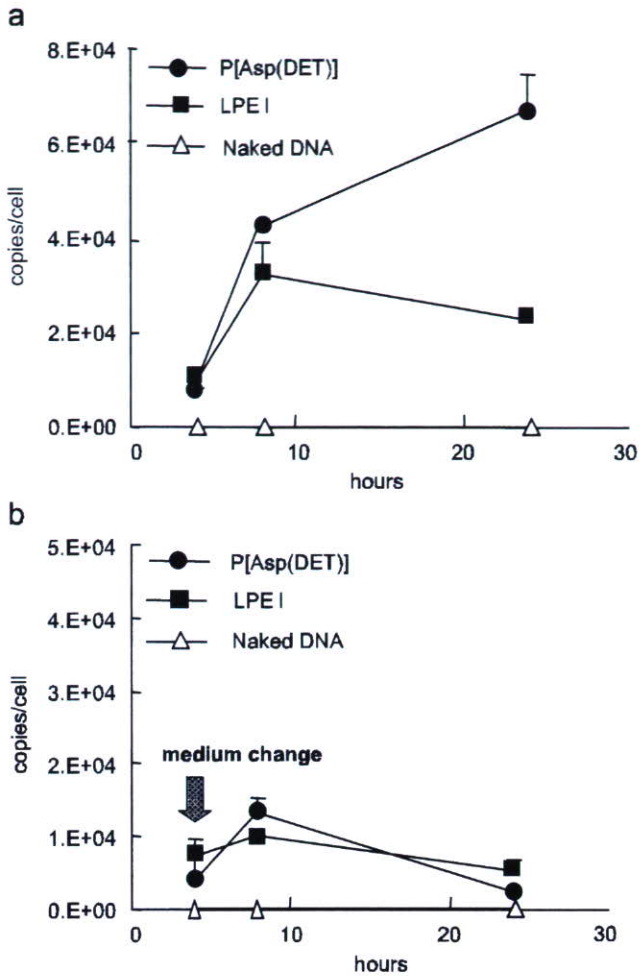

Fig. 3. Evaluation of pDNA uptake after transfecton using P[Asp(DET)] (closed circle), LPEI (closed square), or by the form of naked pDNA (open triangle). The cellular uptake of pDNA was quantified by a PCR, (a) without changing medium during the procedure, or (b) with medium change after 4 h of transfection. Each data represents mean ± SD ($n = 3$).

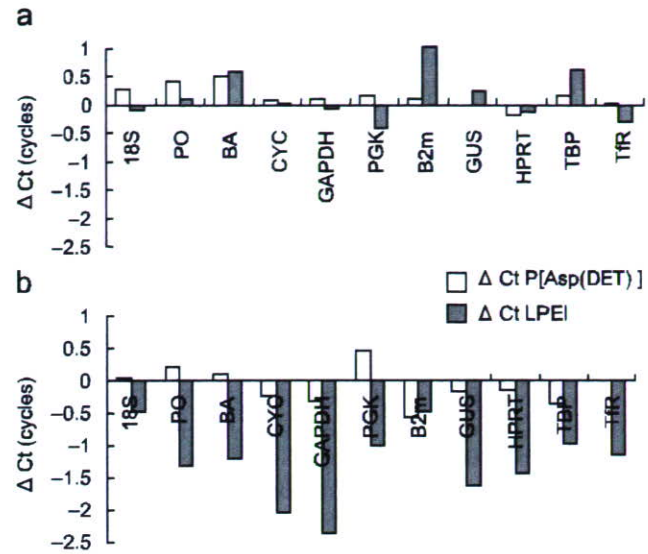

Fig. 4. Housekeeping genes expression after transfection. The mRNA expressions of various housekeeping genes were evaluated by a quantitative PCR at (a) 24 h and (b) 72 h after transfection using P[Asp(DET)] (open bar) or LPEI (filled bar).

the time-dependent decrease in the cellular activity to take up the polyplexes caused by the toxicity of LPEI.

To clarify this possible time-dependent influence on the cellular function from the viewpoint of the genomics, we assessed the change in the gene expressions of 11 frequently used housekeeping genes in the presence of the polyplex. These genes usually revealed a uniform expression, but the expression profile may vary in response to various external factors such as stress on the cells [22,23]. Thus, the variation in their expression profile is a good indicator for assessing the cellular function, a possible perturbation in the cellular homeostasis. The quantitative evaluation of the expression of these housekeeping genes by a real-time PCR revealed that the cells transfected by LPEI apparently showed downregulation in the expression of the housekeeping genes at 72 h after the transfection (Fig. 4(b)). Although the measurement at 24 h showed minimal fluctuation in the housekeeping gene expression, GAPDH and CYC were significantly downregulated by more than two cycles of ΔC_T values compared to those of the control cells at 72 h, indicating a four-fold decrease in gene expression. In these assays, the culture medium was changed at 24 h. Thus, it is likely that LPEI associated with the cells may induce the perturbed gene expression through the continuous interaction with intracellular components even after the medium change at 24 h to remove excess polyplexes in the medium. In contrast, the expression of these genes in the cells transfected by P[Asp(DET)] retained constant even after 72 h, all of which were within 0.5 cycles compared to those of the control cells. These results of the housekeeping gene expressions suggest the sustained homeostasis through the transfection process using P[Asp(DET)], leading to constant cellular activity such as the polyplex uptake (Fig. 3(a)), proliferation (Fig. 1(c)), and continuous gene expression (Fig. 1(b)).

As was occasionally reported, polyplexes induce critical cytotoxicity especially at higher N/P ratios, presumably due to the presence of free polymers [24–26]. Although the mechanisms are likely to involve various cellular responses such as immunostimulation [27] and apoptosis [15,28], the plasma membrane perturbation associated with the cationic polymers may be an initial event that induces the toxicity [28,29]. From our present results on LDH release (Fig. 2), the disorder on the plasma membrane seems to occur within 24 h after the transfection with the LPEI polyplex. In addition, the intracellular events that were noticed as the change in the endogenous gene expressions emerged after 72 h of transfection. It should be noted that these events of the perturbed expression of endogenous genes were inevitable even after further supply of the polyplexes was halted by the medium change at 24 h, strongly suggesting that the free PEI remaining inside the

cells after the polyplex dissociation may cause an unfavorable interaction with the intracellular components in a time-dependent manner.

3.3. Transfection toward mouse calvarial cells and induction of osteogenic differentiation

The data so far indicates the minimal cytotoxicity of P[Asp(DET)], suggesting a feasible capacity in gene delivery for therapeutic purposes. To assess this feasibility, we evaluated the induction of cell differentiation by exogenous gene introduction. pDNAs encoding bioactive factors, caALK6 and Runx2, both of which were revealed to induce the effective osteogenic differentiation [30], were introduced in this way to mouse calvarial cells derived from neonatal calvariae. The osteogenic differentiation was evaluated by the expression of osteocalcin mRNA, a specific osteoblast-differentiation marker. As shown in Fig. 5, the time-dependent increase in osteocalcin expression was confirmed after the transfection of caALK6+Runx2 using P[Asp(DET)]. In contrast, no sign of the osteocalcin expression was observed by the LPEI polyplex until Day 11. Notably, the GFP-encoding pDNA, a negative control of differentiation, achieved almost identical GFP expression by the P[Asp(DET)] and LPEI polyplexes, without apparent morphologic changes in the targeted cells as observed under the microscope (data not shown). It can be reasonably assumed that, with the same transfection procedure, the osteogenic factors of caALK6 and Runx2 were also expressed similarly inside the targeted cells by the P[Asp(DET)] and LPEI polyplexes. Therefore, the lack of osteocalcin induction by the LPEI polyplex is considered to be due to the adverse effect on cell bioactivity by LPEI. In contrast, P[Asp(DET)] was revealed to be available for practical use in the induction of cell differentiation.

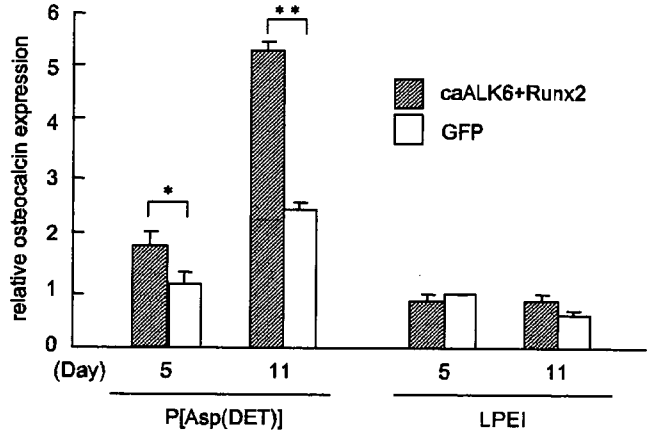

Fig. 5. Evaluation of osteocalcin mRNA expression by a quantitative PCR. Osteogenic differentiation was induced on the mouse calvarial cells by transfection of caALK6 and Runx2 (hatched bar) using P[Asp(DET)] or LPEI. As a negative control, a GFP (open bar) gene was used. After 5 or 11 days of transfection, the total RNA was collected and the osteocalcin expression was estimated. Each data represents mean ± SD ($n = 3$). $^{*}P<0.05$ and $^{**}P<0.01$.

4. Conclusions

In conclusion, although LPEI has been widely used for gene introduction to various cell lines, the time-dependent cytotoxicity, which perturbs cellular homeostasis, should be carefully considered even though an appreciable expression of the reporter gene was achieved. As exemplified here in the osteogenic differentiation, impaired cellular function gave a negative effect in the intracellular signal transduction directing cell differentiation. This aspect of toxicity should be carefully counted especially when gene therapy is proposed to promote such cell functions as differentiation. Worth noting in this regard is the excellent capacity of the gene introduction of P[Asp(DET)] with minimal toxic effects, indicating that this system holds much promise for the therapeutic applications of gene therapy requiring safe and regulated gene expressions.

Acknowledgments

We thank Dr. M. Krüppel and Dr. K. Miyazono for pDNAs expressing caALK6 and Runx2, respectively. This work was supported by Grants-in-Aid for Scientific Research from the Japanese Ministry of Education, Culture, Sports, Science and Technology (#15390452 and #17390412), Health Science Research Grants from the Japanese Ministry of Health, Labor and Welfare (#H17-Immunology-009), and the Core Research Program for Evolutional Science and Technology (CREST) from the Japan Science and Technology (JST) Agency.

References

[1] Marshall E. Gene therapy death prompts review of adenovirus vector. Science 1999;286(5448):2244 5.
[2] Hollon T. Researchers and regulators reflect on first gene therapy death. Nat Med 2000;6(1):6.
[3] Assessment of adenoviral vector safety and toxicity: report of the National Institutes of Health Recombinant DNA advisory committee. Hum Gene Ther 2002;13(1):3 13.
[4] Gansbacher B. Report of a second serious adverse event in a clinical trial of gene therapy for X-linked severe combined immune deficiency (X-SCID). Position of the European Society of Gene Therapy (ESGT). J Gene Med 2003;5(3):261 2.
[5] Mosmann T. Rapid colorimetric assay for cellular growth and survival: application to proliferation and cytotoxicity assays. J Immunol Methods 1983;65(1 2):55 63.
[6] Duncan R. The dawning era of polymer therapeutics. Nat Rev Drug Discov 2003;2(5):347 60.
[7] Omidi Y, Hollins AJ, Benboubetra M, Drayton R, Benter IF, Akhtar S. Toxicogenomics of non-viral vectors for gene therapy: a microarray study of lipofectin- and oligofectamine-induced gene expression changes in human epithelial cells. J Drug Target 2003;11(6): 311 23.
[8] Kabanov AV, Batrakova EV, Sriadibhatla S, Yang Z, Kelly DL, Alakov VY. Polymer genomics: shifting the gene and drug delivery paradigms. J Control Release 2005;101(1-3):259 71.

[9] Kanayama N, Fukushima S, Nishiyama N, Itaka K, Jang WD, Miyata K, et al. A PEG-based biocompatible block catiomer with high buffering capacity for the construction of polyplex micelles showing efficient gene transfer toward primary cells. Chem Med Chem 2006;1(4):439 44.

[10] Boussif O, Lezoualc'h F, Zanta MA, Mergny MD, Scherman D, Demeneix B, et al. A versatile vector for gene and oligonucleotide transfer into cells in culture and in vivo: polyethylenimine. Proc Natl Acad Sci USA 1995;92(16):7297 301.

[11] Boletta A, Benigni A, Lutz J, Remuzzi G, Soria MR, Monaco L. Nonviral gene delivery to the rat kidney with polyethylenimine. Hum Gene Ther 1997;8(10):1243 51.

[12] Goula D, Benoist C, Mantero S, Merlo G, Levi G, Demeneix BA. Polyethylenimine-based intravenous delivery of transgenes to mouse lung. Gene Ther 1998;5(9):1291 5.

[13] Akagi D, Oba M, Koyama H, Nishiyama N, Fukushima S, Miyata T, et al. Biocompatible micellar nanovectors achieve efficient gene transfer to vascular lesions without cytotoxicity and thrombus formation. Gene Ther 2007;14(13):1029 38.

[14] Itaka K, Ohba S, Chung U, Kataoka K. Bone regeneration by regulated in vivo gene transfer using biocompatible polyplex nanomicelles. Mol Ther 2007; Epub ahead of print.

[15] Moghimi SM, Symonds P, Murray JC, Hunter AC, Debska G, Szewczyk A. A two-stage poly(ethylenimine)-mediated cytotoxicity: implications for gene transfer/therapy. Mol Ther 2005;11(6):990 5.

[16] Lehmann MJ, Sczakiel G. Spontaneous uptake of biologically active recombinant DNA by mammalian cells via a selected DNA segment. Gene Ther 2005;12(5):446 51.

[17] Varga CM, Tedford NC, Thomas M, Klibanov AM, Griffith LG, Lauffenburger DA. Quantitative comparison of polyethylenimine formulations and adenoviral vectors in terms of intracellular gene delivery processes. Gene Ther 2005;12(13):1023 32.

[18] Hama S, Akita H, Ito R, Mizuguchi H, Hayakawa T, Harashima H. Quantitative comparison of intracellular trafficking and nuclear transcription between adenoviral and lipoplex systems. Mol Ther 2006;13(4):786 94.

[19] Itaka K, Harada A, Yamasaki Y, Nakamura K, Kawaguchi H, Kataoka K. In situ single cell observation by fluorescence resonance energy transfer reveals fast intra-cytoplasmic delivery and easy release of plasmid DNA complexed with linear polyethylenimine. J Gene Med 2004;6(1):76 84.

[20] Goncalves C, Pichon C, Guerin B, Midoux P. Intracellular processing and stability of DNA complexed with histidylated polylysine conjugates. J Gene Med 2002;4(3):271 81.

[21] Lechardeur D, Sohn KJ, Haardt M, Joshi PB, Monck M, Graham RW, et al. Metabolic instability of plasmid DNA in the cytosol: a potential barrier to gene transfer. Gene Ther 1999;6(4): 482 97.

[22] Thellin O, Zorzi W, Lakaye B, De Borman B, Coumans B, Hennen G, et al. Housekeeping genes as internal standards: use and limits. J Biotechnol 1999;75(2-3):291 5.

[23] Jain M, Nijhawan A, Tyagi AK, Khurana JP. Validation of housekeeping genes as internal control for studying gene expression in rice by quantitative real-time PCR. Biochem Biophys Res Commun 2006;345(2):646 51.

[24] Godbey WT, Wu KK, Mikos AG. Poly(ethylenimine)-mediated gene delivery affects endothelial cell function and viability. Biomaterials 2001;22(5):471 80.

[25] Morimoto K, Nishikawa M, Kawakami S, Nakano T, Hattori Y, Fumoto S, et al. Molecular weight-dependent gene transfection activity of unmodified and galactosylated polyethyleneimine on hepatoma cells and mouse liver. Mol Ther 2003;7(2):254 61.

[26] Boeckle S, von Gersdorff K, van der Piepen S, Culmsee C, Wagner E, Ogris M. Purification of polyethylenimine polyplexes highlights the role of free polycations in gene transfer. J Gene Med 2004; 6(10):1102 11.

[27] Regnstrom K, Ragnarsson EG, Koping-Hoggard M, Torstensson E, Nyblom H, Artursson P. PEI-a potent, but not harmless, mucosal immuno-stimulator of mixed T-helper cell response and FasL-mediated cell death in mice. Gene Ther 2003;10(18): 1575 83.

[28] Florea BI, Meaney C, Junginger HE, Borchard G. Transfection efficiency and toxicity of polyethylenimine in differentiated Calu-3 and nondifferentiated COS-1 cell cultures. AAPS PharmSci 2002;4(3):E12.

[29] Hunter AC. Molecular hurdles in polyfectin design and mechanistic background to polycation induced cytotoxicity. Adv Drug Deliv Rev 2006;58(14):1523 31.

[30] Ohba S, Ikeda T, Kugimiya F, Yano F, Lichtler A, Nakamura K, et al. Identification of a potent combination of osteogenic genes for bone regeneration using embryonic stem (ES) cell-based sensor. FASEBj 2007;21(8):1777 87.

Available online at www.sciencedirect.com
ScienceDirect
Reactive & Functional Polymers 67 (2007) 1361–1372
REACTIVE & FUNCTIONAL POLYMERS
www.elsevier.com/locate/react

Study of the quantitative aminolysis reaction of poly(β-benzyl L-aspartate) (PBLA) as a platform polymer for functionality materials

Masataka Nakanishi [a], Joon-Sik Park [b], Woo-Dong Jang [c], Makoto Oba [d], Kazunori Kataoka [a,b,*]

[a] *Department of Materials Engineering, Graduate School of Engineering, The University of Tokyo, 7-3-1 Hongo, Bunkyo, Tokyo 113-8656, Japan*
[b] *Center for Disease Biology and Integrative Medicine, Graduate School of Medicine, The University of Tokyo, 7-3-1 Hongo, Bunkyo, Tokyo 113-0033, Japan*
[c] *Department of Chemistry, College of Science, Yonsei University, 134 Sinchondong, Seodaemun-gu, Seoul 120-749, Republic of Korea*
[d] *Department of Clinical Vascular Regeneration, Graduate School of Medicine, The University of Tokyo, 7-3-1 Hongo, Bunkyo, Tokyo 113-8655, Japan*

Received 30 June 2007; received in revised form 31 July 2007; accepted 2 August 2007
Available online 29 August 2007

Dedicated to Professor Teiji Tsuruta on the occasion of his 88th birthday (Beiju).

Abstract

A facile and quantitative aminolysis of poly(β-benzyl L-aspartate) (PBLA) as well as the solution properties of the prepared cationic polyaspartamide were investigated in this study. The reaction was found to proceed in good yield without undesired side reactions via the formation of a succinimide intermediate in the polymer backbone, which was efficiently converted to polyaspartamide accompanying the α,β isomerization of the main chain. The polarity of solvents and the secondary structure of the polymer strand were closely related to each other in terms of reactivity and stereoselectivity. The aminolysis of PBLA treated with one equivalent amine against benzyl ester groups resulted in the complete conversion at 35 °C in random-coil solvents within 1 h. The racemization that accompanied this reaction was observed in random-coil solvents, but was efficiently suppressed in helicogenic solvents, with 95% of the optical purity maintained in CH_2Cl_2. In addition, the quantitative introduction of *N*,*N*-diisopropylethylenediamine (DIP) led to the formation of cationic polyaspartamide, poly[*N*-(*N*′,*N*′-diisopropylaminoethyl)aspartamide] (PAsp(DIP)), which showed pH and thermo-sensitivities in aqueous media. This systematic investigation of the aminolysis of PBLA with DIP demonstrates the feasibility of a PBLA-aminolysis system for designing functionalized polyaspartamides which can be useful as biomaterials.

Keywords: PBLA; Aminolysis; Quantitative side-chain reaction; Succinimide; Suppression of racemization; pH and thermo-sensitivities

* Corresponding author. Address: Department of Materials Engineering, School of Engineering, The University of Tokyo, Japan. Tel.: +81 3 5841 7138; fax: +81 3 5841 7139.
E-mail address: kataoka@bmw.t.u-tokyo.ac.jp (K. Kataoka).

1381-5148/$ - see front matter © 2007 Elsevier Ltd. All rights reserved.
doi:10.1016/j.reactfunctpolym.2007.08.009

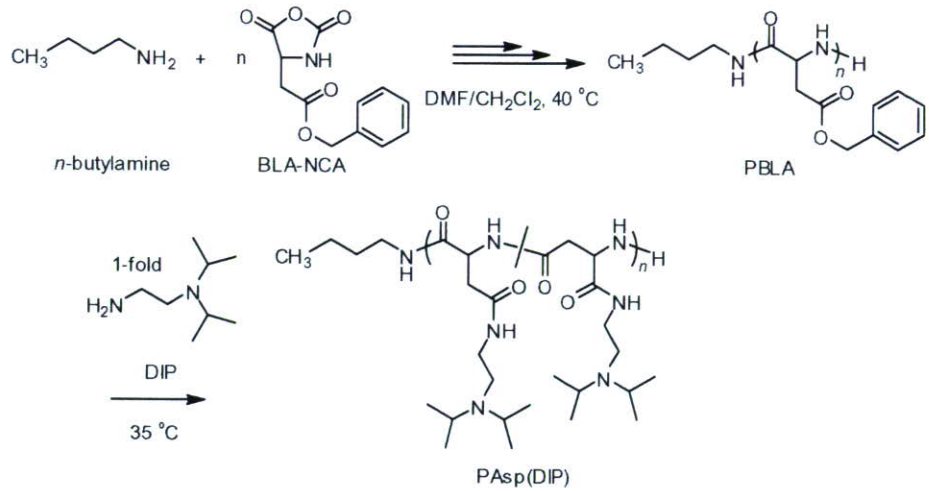

Scheme 1. Synthetic procedures of PBLA and PAsp(DIP) by the successive aminolysis reaction of PBLA.

1. Introduction

Chemical modification by the side-chain reaction of polymer is a convenient way to prepare a variety of functionalized derivatives from a single platform polymer [1–3]. For example, the precursor polymers bearing functional groups such as active ester [4–9], (meth)acryl chloride [10–12], and alkyne [13,14] are typical representatives with a potential for further functionalization or versatile modification according to particular applications. As a rule, the side-chain reaction was considered a facile synthetic route to obtaining polymer analogues with a constant degree of polymerization (DP) and molecular weight distribution (MWD) from a single platform polymer. Thus, the use of precursor polymer as a common intermediate allows for combinatorial strategies, feasible for evaluating and optimizing the correlation between the polymer structure and function.

There have also been many examples in bio-related fields where poly(amino acid)s with high biocompatibility and low toxicity [15–18] were chemically modified to increase their feasibility by binding hydrophobic drugs [19], a hydrophilic ethylene glycol segment [20] and pilot molecules [21] into the side chain. Although there have been several studies on side-chain modification using poly(lysine) or poly(glutamate/aspartate) as a platform polymer, the side-chain reaction of these poly(amino acid)s does not proceed quantitatively. The conversion of all the flanking moieties of the precursor polymers requires extreme conditions such as a high concentration of reactant, high temperature and long reaction time, leading to side reactions such as the decrease of molecular weight (MW) by the cleavage of the amide linkages in the main-chain, as in the case of the aminolysis of Poly(γ-benzyl L-glutamate) (PBLG) [22,23]. Alternatively, poly(succinimide) has been investigated as a more active precursor to preparing the isomeric library of polyaspartamide by the quantitative introduction of the functional groups [24–29]. However, the synthesis of this active precursor has some drawbacks, including a long time reaction, high reaction temperature, and coloring of the obtained product [30,31], limiting the resultant polymer under control. Namely, the polymers are still highly heterogeneous, not only in terms of DP and MWD but also in terms of optical purity and composition of the functional units in the side chain [32,33].

In this regard, we have recently established that the flanking benzyl ester groups of poly(β-benzyl L-aspartate) (PBLA) undergo a quantitative aminolysis reaction with various primary amine compounds, thus offering a variety of polyaspartamides useful for designing polymeric micelles and vesicles as a biomaterial application [34–39]. Although it has been suggested that the mechanism of this unique aminolysis reaction is involved with the succinimidyl ring formation, the details have not yet been clarified. Thus, it is critical to obtain insight into the reaction mechanism, particularly from the standpoint of kinetics, and to identify the detailed structure of polyaspartamide in order to assess its feasibility for use as biomaterials. To this aim, we investigated the mechanism and kinetics of the aminolysis reaction of PBLA, focusing on both the α to β transition

and racemization relevant to the solvent effect and the higher-ordered structure of polymer strands.

In this study, the cationic polyaspartamide was synthesized by reacting PBLA with *N*,*N*-diisopropylethylenediamine (DIP), and its solubility behavior responsive to pH and temperature was investigated. DIP was selected as a nucleophile to study the aminolysis mechanism and the environmentally responsive properties of polyaspartamide. The primary amino group of DIP was converted to the amide group after the aminolysis of PBLA, and the *N*,*N*-diisopropylaminoethyl group of DIP was responsible for pH- and thermo-sensitivities (Scheme 1). Among several alkyl groups as a hydrophobic moiety, the isopropyl group was selected with the expectation that a sharp transition of the polymer in aqueous media, like the typical thermoresponsive polymer, poly(*N*-isopropylacrylamide) [40], would occur. In addition, the tertiary amino group with two neighboring isopropyl groups was also selected not only for the hydrophobic-hydrophilic balance between the ionic segment and alkyl segment, but also to exclude undesired cross-linking during the aminolysis. Concerning the kinetics, in general the reactivity of side chains can be controlled not only by the polarity of the solvent but also by the polymer conformation depending on the solvation of side groups, steric hindrances, and the distance of the vicinal groups. From this point of view, we conducted this study in a comparable solvent system for the purpose of evaluating each effect of solvent polarity and polymer conformation on the kinetics and racemization.

2. Experimental

2.1. Materials

β-Benzyl L-aspartate *N*-carboxy-anhydride (BLA-NCA) was obtained from Nippon Oil and Fats (Tokyo, Japan). *N*,*N*-Dimethylformamide (DMF), 1,4-dioxane (dioxane), dimethylsulfoxide (DMSO), dichloromethane (CH_2Cl_2), and chloroform ($CHCl_3$) were purchased from Wako Pure Chemical Industries (Osaka, Japan) and were purified by distillation according to the conventional procedure [41]. *N*,*N*-Diisopropylethylenediamine (DIP), *n*-butylamine and triethylamine (TEA) were purchased from Tokyo Kasei Kogyo (Tokyo, Japan) and were distilled from calcium hydride under reduced pressure. The other chemicals were used as received.

2.2. Method

The ^{1}H NMR spectrum was recorded on a JEOL EX 300 spectrometer (JEOL, Tokyo, Japan) at 300 MHz. Chemical shifts were reported in parts per million (ppm) downfield from tetramethylsilane. MW and MWD were estimated using a gel-permeation chromatography (GPC) (TOSOH HLC-8220) system equipped with two TSK gel columns (TSK-gel Super AW4000 and Super AW3000) and an internal refractive index (RI) detector. The columns were eluted with *N*-methyl-pyrrolidone (NMP) containing lithium bromide (50 mM) (0.3 ml min^{-1}) at 40 °C. MW were calibrated with poly(ethylene glycol) standards (Polymer Laboratories, Ltd., UK). The IR spectra were obtained with an IR-550 JASCO spectrophotometer. Gas chromatography (GC) was carried out with GC17A (SHIMADZU, Tokyo, Japan) gas chromatograph equipped with a 30-m long, 250 μm i.d., open tubular column, DB-1 (SHIMADZU GLC, Tokyo, Japan), and a flame ionization detector. C-R7A (SHIMADZU, Tokyo, Japan) was used for instrument control and data acquisition. The carrier gas was hydrogen. The pressure at the head of the column was 400 kPa, and the linear velocity at the end of the column was 41 cm s^{-1}. The sample was injected onto the column at a split ratio of over 25:1. The injection port temperature was 200 °C.

2.3. Synthesis of poly(β-benzyl L-aspartate) (PBLA)

To obtain PBLA (Scheme 1), BLA-NCA (2.49 g, 10 mmol) was polymerized in the mixture of DMF (10.0 mL) and CH_2Cl_2 (100 mL) at 40 °C by the initiation from the terminal primary amino group of *n*-butylamine (14.6 mg, 200 μmol). PBLA was purified by precipitation in ether (3 L) three times, and was confirmed to have a unimodal MWD (M_w/M_n: 1.07) by GPC measurement (Fig. 1C). The DP of PBLA was calculated to be 52 based on ^{1}H NMR spectroscopy (Fig. 1A).

2.4. Synthesis of poly[N-(N′,N′-diisopropylaminoethyl)aspartamide] (PAsp(DIP))

Lyophilized PBLA (202 mg, 20 μmol) was dissolved in DMSO (10 mL), followed by the reaction with 1-fold DIP (1 equiv to the residual benzyl ester group in PBLA, 144.3 mg, 1 mmol) under mild anhydrous conditions at 35 °C for 1 h to obtain

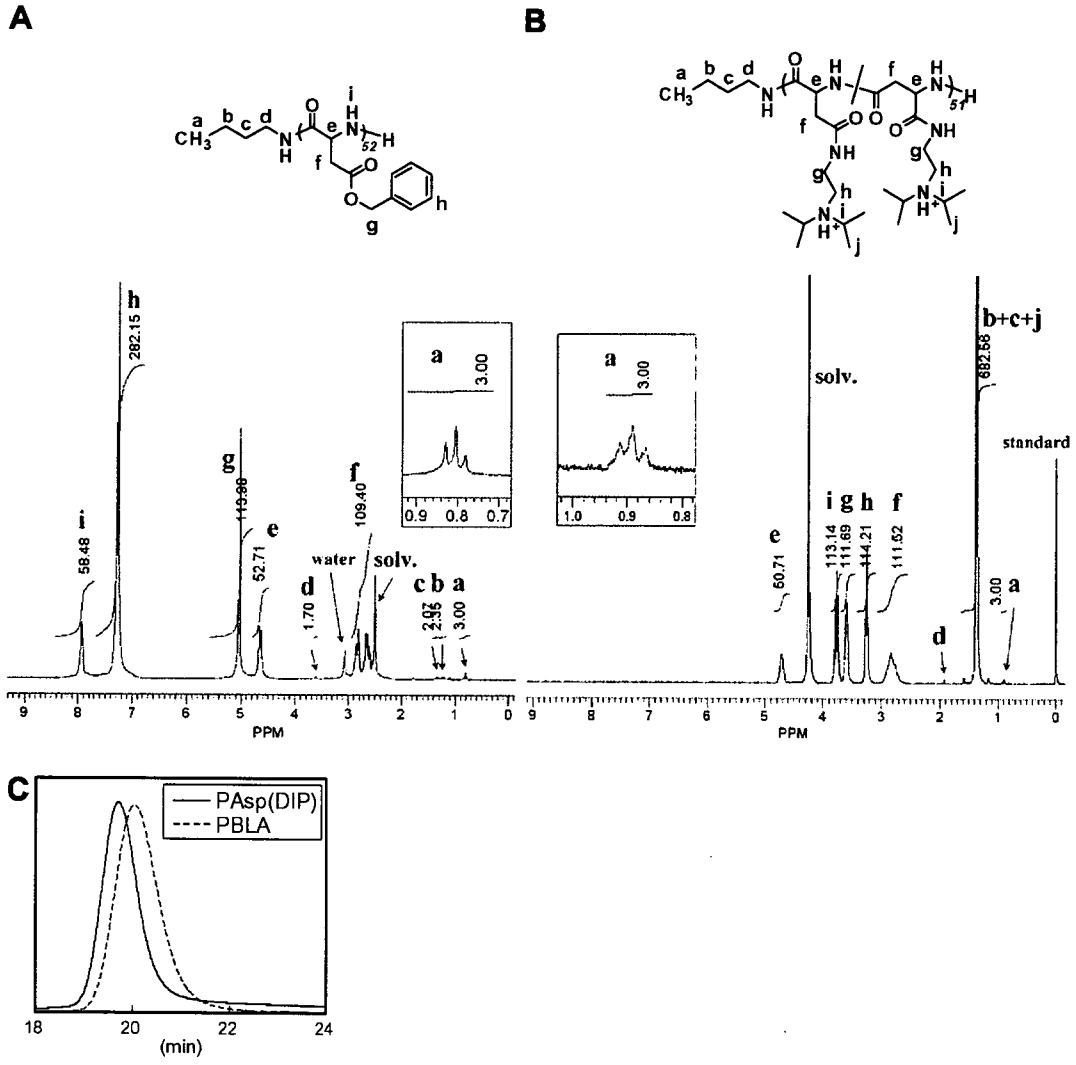

Fig. 1. ^{1}H NMR spectra of (A) PBLA in DMSO-d_6 at 50 °C and (B) PAsp(DIP) synthesized in DMSO in D_2O at 80 °C. (C) GPC diagrams of PBLA and PAsp(DIP) (PEG standard, eluent: NMP (containing 50 mM LiBr), temperature 40 °C, RI detection).

PAsp(DIP). After the reaction, the reaction mixture was slowly added dropwise into a cooled aqueous solution of acetic acid (10% v/v, 40 mL) and dialyzed against an aqueous solution of 0.01 N HCl three times and distilled water one time (molecular weight cut off: 3500 Da). The final solution was lyophilized to obtain the polymer in the chloride salt form with a yield of 92% (221 mg). In addition to the chloride salt form, the unprotonated PAsp(DIP)s were obtained as follows. The reaction mixture was purified by dialysis against DMSO three times and methanol three times. The solution was evaporated *in vacuo* and the polymer was dissolved in benzene, followed by lyophilization. The unprotonated PAsp(DIP) was then obtained as a white powder with a yield of 90% (215 mg). Similarly, the aminolysis of PBLA with DIP was carried out at 35 °C in NMP (reaction time: 1 h), DMF (reaction time: 1 h), $CHCl_3$ (reaction time: 200 h) and CH_2Cl_2 (reaction time: 160 h), respectively. In the case of dioxane, the solution of PBLA in dioxane was at first completely dissolved at 50 °C and then the temperature was allowed to decrease the temperature to 35 °C, followed by the reaction with an equivalent DIP for 260 h. All the yields were approximately 90%. The completion of the aminolysis reaction was confirmed by GC.

2.5. Reaction velocity measurements

The aminolysis of PBLA was carried out using an equivalent DIP at 35 °C in a comparable solvent sys-

tem. The conversion of the BLA residue into the aspartamide residue was calculated from both the remaining amount of DIP and the amount of the benzyl alcohol. The remaining amount of DIP was measured using GC with the internal reference method using *n*-decane as internal standard. PBLA (202 mg) was reacted with 1-fold DIP (144 mg) in 10 mL of solvent. The rate of debenzylation was determined by comparison of the intensity of CH_2 of the leaving benzyl alcohol with that of benzyl ester based on ^{1}H NMR spectroscopy using DMSO-d_6 and CD_2Cl_2 as solvent. PBLA (20.2 mg) was reacted with DIP (14.4 mg) in 1 mL of solvent at 35 °C during the ^{1}H NMR measurement.

2.6. Optical rotation measurements

The specific optical rotation measurements of the polymer samples were carried out in CH_2Cl_2 and DMSO respectively, using a digital polarimeter DIP-370 (JASCO) at a 546 nm wavelength, with a cell of 100 mm length and an integration time of 30 s. The concentration of polymer was adjusted to 1.0 wt% for all the measurements. $[\alpha]_D$ was measured at definite time intervals after adding 1-fold DIP. The measurement was done 20 times for each sample to obtain the average value.

2.7. Analysis of aspartamide enantiomers

The D/L-aspartamide ratios were determined by high performance liquid chromatography carried out by the HiPep Laboratories (Kyoto, Japan) using the enantiomer labeling method (ELAB). This analysis was conducted using a fully automated D/L and quantitative amino acid analyzer, a Shimadzu-CAT Model DLAA-1, which consists of an automated derivatizer with a robot arm, Autoderivat 100/2 of CAT, and a gas chromatograph, Shimadzu Model GC/DLAA with an auto injector, AOC/DLAA, in combination with a chromatographic data processor, Shimadzu Chromatopac C-R4A [42].

2.8. Potentiometric titration and transmittance measurements

PAsp(DIP) (30 mg) prepared in DMF was dissolved in 50 mL 0.01 N HCl and titrated with 0.01 N NaOH added in quantities of 0.063 mL after the pH values were stabilized (minimal interval: 30 s), using an automatic titrator (TS-2000, Hiranuma, Kyoto, Japan) for the titration and transmittance measurements. The pH values and transmittance were measured at 10 °C, 20 °C, 30 °C, 40 °C and 50 °C. The α/pH curves were determined from the titration curves obtained. Each calibration was carried out at the same temperature as each measurement.

3. Results and discussion

3.1. Preparation of PAsp(DIP)

PBLA is known to form the left-handed α-helix in apolar solvents such as dioxane [43], $CHCl_3$ [44], CH_2Cl_2 [45] and the random-coil in polar solvents such as DMF [46] and DMSO [43]. Because of this, these five random-coil and helicogenic solvents with various dielectric constants were selected for this study.

From the ^{1}H NMR measurement, the DP of the PAsp(DIP), comparing the peak intensity ratio of the CH_3 of the *n*-butyl group (**a**) with α-C*H* of PAsp(DIP) (**e**) was calculated to be 51, and it was confirmed that PAsp(DIP) synthesized in DMSO has a unimodal MWD (M_w/M_n: 1.08) by GPC measurement, thus indicating that the aminolysis proceeded quantitatively without causing any cleavage of the main chain (Fig. 1). Similarly, it was confirmed that all the PAsp(DIP)s prepared in other solvents had almost the same MW and a unimodal MWD (Table 1). Therefore, this result demonstrated that the aminolysis of PBLA was a useful side-chain exchanging reaction avoiding the side reaction of the cleavage of the main chain in the appropriate condition.

3.2. Reaction velocity

A significant difference was found in the reaction rate between polar random-coil solvents and apolar helicogenic solvents, as shown in Fig. 2. The reaction was much faster in random-coil solvents than in helicogenic solvents. From a practical point of view, it is worth mentioning that aminolysis with a 1-fold amine is completed after 1 h at 35 °C in polar solvents. In addition, although no difference was found in reactivity among random-coil solvents, the reaction was clearly faster in helicogenic solvents with the increasing dielectric constant of the solvent, suggesting that the rate of the aminolysis reaction of PBLA also depends on the polarity of the solvents. The results of the kinetic studies show that the aminolysis of side-

Table 1
Analytical data of M_w/M_n and L-isomer (%) of PAsp(DIP) synthesized in various solvents

Polymer solvent	PBLA	PAsp(DIP)				
		Dioxane	$CHCl_3$	CH_2Cl_2	DMF	DMSO
ε[a]		2.2	4.8	9.1	37	47
M_w/M_n[b]	1.07	1.08	1.07	1.08	1.09	1.08
L (%)[c]	99.9	83.8	89.0	94.5	72.7	73.6

[a] Indicates the dielectric constant of the solvent.
[b] Determined by GPC.
[c] Determined by ELAB method carried out by HiPep laboratories.

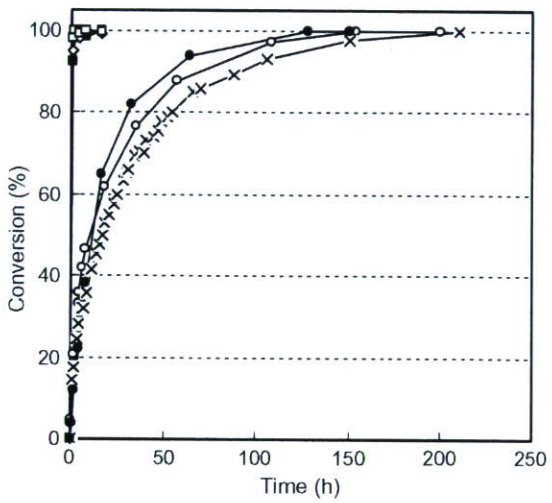

Fig. 2. Time profile of the conversion rate calculated from the remaining DIP in DMSO (□), DMF (◇), CH_2Cl_2 (○) and $CHCl_3$ (×) and the leaving benzyl alcohol in DMSO-d_6 (■) and CD_2Cl_2 (●) in the condition where PBLA reacts with 1-fold DIP at 35 °C.

chain esters of PBLA can be greatly affected by both the conformation of the polymer strand and the polarity of the solvents.

The kinetics data described above suggest that there could be an active intermediate to have this reaction progress rapidly and quantitatively, because the aminolysis of esters, in other words, a way of directly transforming esters to amides, usually requires stoichiometric amounts of promoters or metal mediators [47]. It has been reported that a large amount of primary amines was required to modify all the flanking esters in the side chain of PBLG by aminolysis, and that main-chain scission caused due to the aminolysis of the amide linkage in the main chain by the remaining primary amines [22,23]. In contrast, the stoichiometric aminolysis reaction of PBLA resulted in the prompt and complete conversion in polar and apolar solvents under a mild condition. Of interest is the significant difference in the reaction rate between PBLA and PBLG, because the difference between their primary structures is the presence or absence of γ-CH_2 in the side chain. Blout et al. [46] reported the formation of poly(succinimide), an active precursor polymer, from PBLA when PBLA was treated with catalytic amounts of base in DMF or DMSO. The formation of poly(succinimide) was determined by isolation and comparison with the infrared spectra reported in the literature [46]. However, the treatment of PBLG under identical conditions showed no evidence of cyclization to poly(glutarimide) [46]. Therefore, the mechanism by which α to β isomerization of aspartic acid occurs was focused here in order to understand the mechanism by which the aminolysis of PBLA occurs. Moreover, there have been many reports showing that the racemization of aspartic acid and asparagine residues was accelerated via succinimide intermediates [48–53]. From this result, it is highly expected that the racemization occurs when the succinimide formation occurs.

For the reasons mentioned above, it is estimated that there are three stages: (1) ring formation, (2) racemization, (3) aminolysis in the present reaction of PBLA (Scheme 2). The reaction rate constants of each stage were defined as k_1, k_2 and k_3, respectively. In the first stage, the aminolysis of PBLA starts with the activation of the nitrogen atom in the main chain by an amine as a weak base coordinating the proton of the amide group, and then the nucleophilic attack by the activated nitrogen on the carbon atom of the carbonyl group in the side chain occurs to form the succinimidyl ring. The eliminated proton which recombines with the benzyloxyl group is released as benzyl alcohol, accompanying the regeneration of amine. Therefore, the ring formation is expected to be a catalytic reaction. In the second stage, the proton in the α-position is easily eliminated with ease in the succinimidyl ring, and then racemization proceeds by the keto–enol tau-

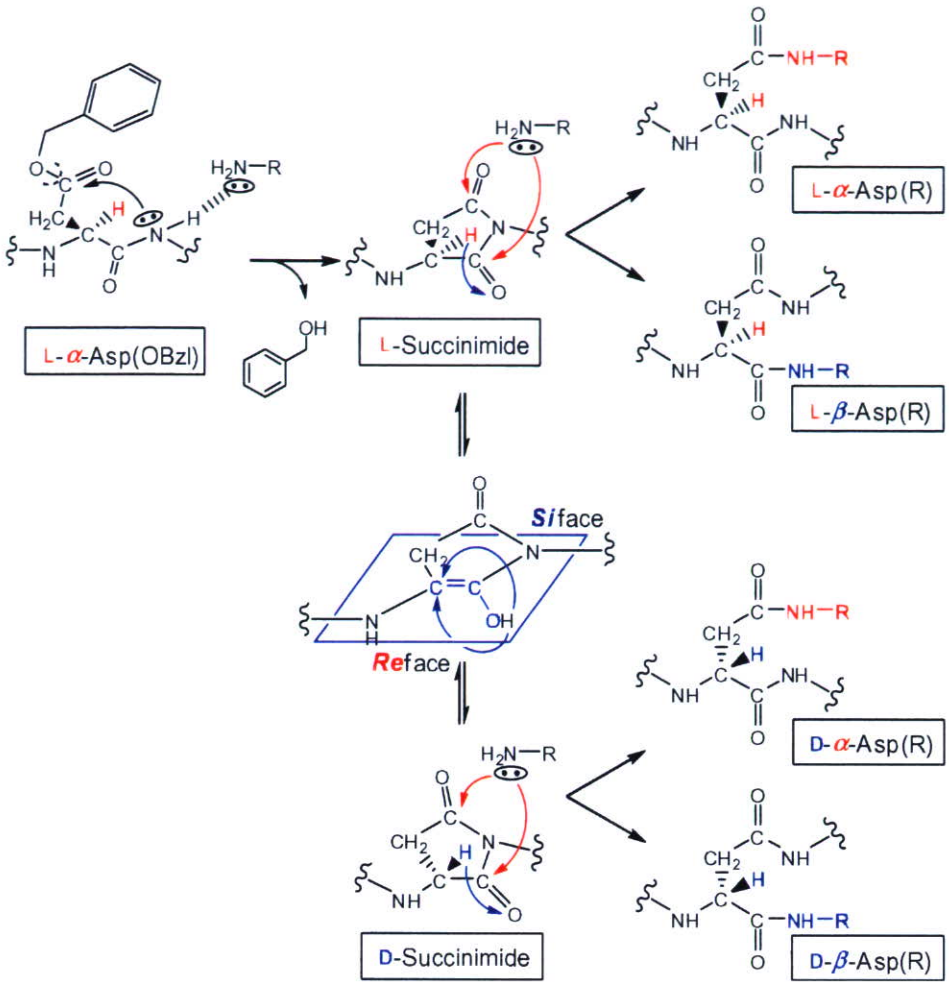

Scheme 2. Mechanism of aminolysis reaction of PBLA.

tomerism. In the third stage, an amine undergoes a nucleophilic attack to one of two carbonyl groups in the succinimidyl ring, which is efficiently converted to the isomerization to form the α,β-aspartamide.

Therefore, the aminolysis of PBLA by less than a 1-fold amount of DIP in DMSO($-d_6$) or CH_2Cl_2 (CD_2Cl_2) was performed to confirm whether aminolysis proceeds via the formation of the succinimide

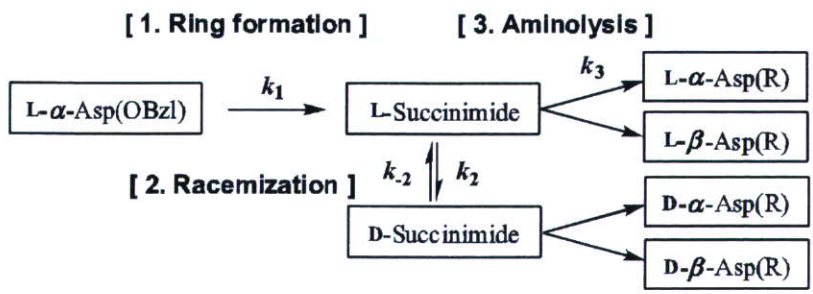

intermediate or not. In addition, the degree of racemization after the aminolysis of PBLA with 1-fold DIP was analyzed.

3.3. Identification of intermediate structure and kinetics

3.3.1. Identification of intermediate structure and kinetics in DMSO

The confirmation of an intermediate structure was done in the condition where PBLA reacted with 0.5-fold DIP in DMSO-d_6 using ^{1}H NMR spectroscopy recorded after 0.5 h, 1 h and 6 h (Fig. 3). It was determined that a 0.5-fold amount of DIP was added to this system by comparing the intensity of CH_3 (**j**) of DIP with that of CH_2 (**c**) of the benzyl group of PBLA. The sharp peak of CH_2 (**f**) of the leaving benzyl alcohol appeared at 4.5 ppm, and the intensity increased promptly in association with the separation of the peak (**d**) due to the benzyl alcohol. The integration value of CH_2 (**f**) of the benzyl alcohol became ca. 2 at 1 h. This is consistent with the complete disappearance of the peak corresponding to CH_2 (**c**) of the benzyl group of PBLA within 1 h. Thus, it was confirmed that the debenzylation was completed within 1 h. It was also confirmed by GC that all the DIP were consumed after 6 h.

Comparing the spectrum of PBLA (A) with that of the reactant at 0.5 h (B) in Fig. 3, it is worth noting the substantial shift of the α-C*H* (**a**) peak at 4.7 ppm. Concomitantly, the peak assigned to β-CH_2 seems to shift from 2.6 and 2.8 ppm (**b**) to 2.7 and 3.2 ppm (**l**), respectively, suggesting the substantial change in the main chain structure. Furthermore, the appearance of new peaks at 5.3 (**k**) and 5.1 (**m**) ppm was clearly observed. For further analysis, each intensity and the summation of the two peaks (**k**) and (**m**) from (B) to (D) in Fig. 3 were compared. According to the reported chemical shift values of poly(succinimide) [54], the peaks (**k**) and (**l**) were assigned to α-C*H* and β-CH_2, respectively, of the succinimide ring produced in the main chain. In accordance with the gradual decrease in the peak intensity of peak (**k**) with time, an alternative increase in the intensity for peak (**m**) was observed, suggesting the progress of the aminolysis reaction. Note that the summation of the peak intensities of (**k**) and (**m**) always took the constant value of 1.1 after 1 h. Therefore, it is reasonable to conclude that the peak (**m**) is assigned to α-C*H* of polyaspartamide. The time-trace of the ^{1}H NMR spectra revealed that the aminolysis reaction successively occurred after the prompt progress of succinimide formation ($k_1 > k_3$) in DMSO.

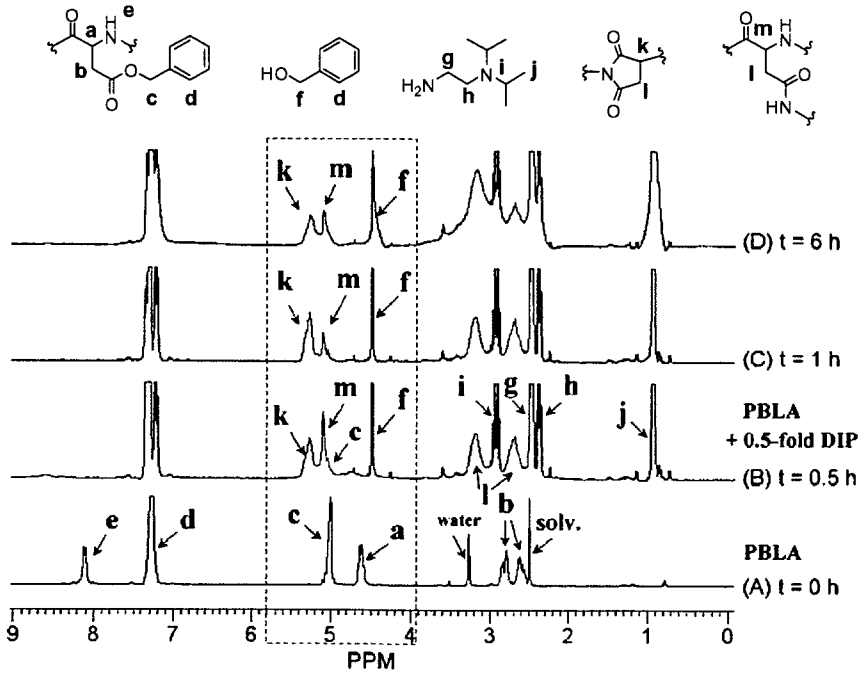

Fig. 3. Time-trace of ^{1}H NMR spectra of PBLA reacting with 0.5-fold DIP in DMSO-d_6 at 35 °C.

Next, an IR measurement was performed to directly detect the succinimide structure in the condition where PBLA reacted with 0.005-fold DIP in DMSO at 35 °C for 30 min. In the IR spectrum of the product, the amide I, amide II and ester peaks almost disappeared and the imide peaks of the succinimidyl ring appeared clearly at 1717 cm^{-1} and 1800 cm^{-1}, as shown in Fig. 4A and B. The IR spectrum of the product was very similar to that of the model imide, *N*-ethyl-succinimide (data not shown) and similar to the spectrum of Poly(succinimide) which has been reported [46]. Therefore, it is reasonable to conclude that DIP catalytically transduces the BLA residue to succinimide, an active intermediate, which then quantitatively converted to aspartamide, and that aspartamide includes β-isomer.

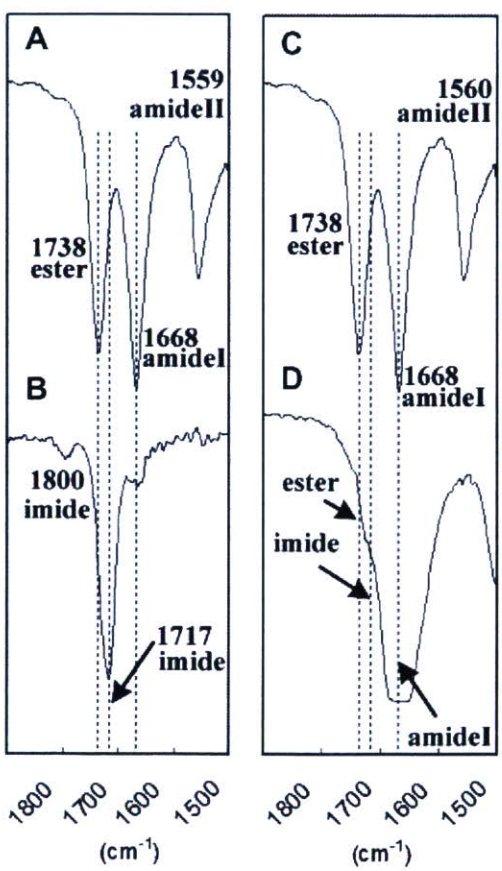

Fig. 4. Infrared absorption spectra with assignments at a range of 1800–1500 cm^{-1} of (A) PBLA, (B) PBLA reacting with 0.005-fold DIP in DMSO for 30 min, (C) PBLA reacting with 0.005-fold DIP in CH_2Cl_2 for 24 h, and (D) PBLA reacting with 1-fold TEA in CH_2Cl_2 for 12 h.

3.3.2. Identification of intermediate structure and kinetics in CH_2Cl_2

Similarly, the identification of an intermediate structure in CH_2Cl_2 was carried out to explore the mechanism involved in the quantitative aminolysis reaction in apolar solvents. The ^1H NMR spectra were obtained in the condition where PBLA reacted with 0.5-fold DIP in CD_2Cl_2 at 35 °C as shown in Fig. 5. The sharp peak of CH_2 (**f**) of the leaving benzyl alcohol appeared at 4.6 ppm with a gradual increase in the intensity, with the reaction time occurring more slowly than that in the DMSO-d_6 system. Eventually, 47% of benzyl alcohol was eliminated in 237 h. Nevertheless, no peak corresponding to succinimide as an intermediate structure was found in the spectra from (A) to (E), unlike in the DMSO-d_6 system. An IR measurement was carried out in the condition where PBLA reacted with the catalytic amount of DIP for 24 h in CH_2Cl_2. The spectrum obtained after 24 h was quite similar to that of PBLA (Fig. 4C) without any sign of succinimide ring formation. Further analysis was then carried out using triethylamine (TEA) as a weak base, which can act as a catalyst leading to formation of the succinimide ring, yet cannot undergo an aminolysis reaction because of the lack of a primary amino group. Eventually, the solution of PBLA reacting with an equivalent TEA for 24 h became turbid, and its IR spectrum clearly included the band assignable to the imide structure (Fig. 4D), indicating the formation of a succinimide structure.

Note that poly(succinimide) is known to be insoluble in CH_2Cl_2 [46], being consistent with the precipitate formation in the reaction mixture of PBLA with TEA in CH_2Cl_2. In the reaction system with DIP, the produced succinimide moiety promptly reacted with the primary amino group of DIP to form an aspartamide with a flanking diisopropylaminoethyl group because the succinimidyl ring formation was the rate-limiting step ($k_1 < k_3$), eventually maintaining the polymer solubility in CH_2Cl_2.

3.4. Stereoselectivity

A measurement of the specific optical rotation was conducted to analyze the racemization and conformational change of the polymer strand during the aminolysis of PBLA. Notably, a significant difference in $[\alpha]_D$ was observed between the polymers dissolved in DMSO and CH_2Cl_2 (Fig. 6). $[\alpha]_D$ of the polymer in DMSO immediately became almost

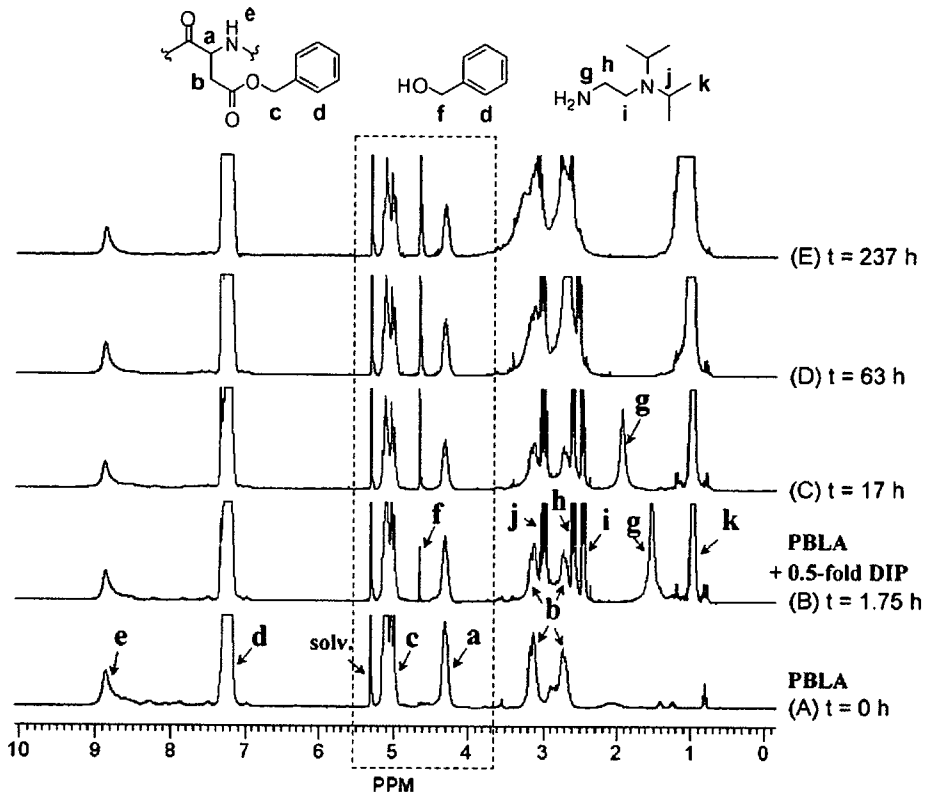

Fig. 5. Time-trace of ^{1}H NMR spectra of PBLA reacting with 0.5-fold DIP in CD_2Cl_2 at 35 °C.

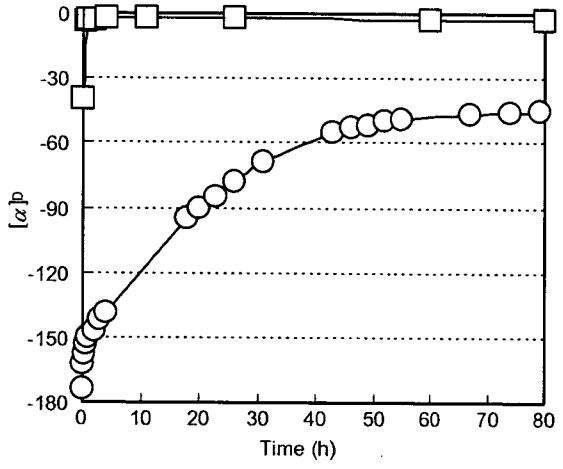

Fig. 6. Time-trace of $[\alpha]_D$ of PBLA reacting with 1-fold DIP at room temperature in DMSO (□) and CH_2Cl_2 (○).

zero after the DIP addition, suggesting the prompt racemization. $[\alpha]_D$ of PBLA in CH_2Cl_2 showed a highly negative value compared to that in DMSO due to the formation of the left-handed α-helix. Then, after the addition of DIP, alternatively, $[\alpha]_D$ of the system revealed a gradual shift in the positive direction and converged from the value of −180 to −45 after 80 h. It should be noted that the $[\alpha]_D$ value of −45 coincided with that for the random coiled PBLA in polar solvents such as DMSO.

Further analysis revealed that racemization occurred in the polar solvents and was effectively prohibited in the apolar solvents (Table 1), indicating that the $k_{2\_apolar\ solvent}$ was quite smaller than the $k_{2\_polar\ solvent}$. It is worth mentioning that the optical purity of the L-isomers was maintained with the yield of 95% in CH_2Cl_2, which is unprecedentedly high.

Racemization occurs by the rearrangement of the eliminated proton in the α position from Si face known as the keto–enol tautomerization (Scheme 2). It is reasonable to assume that the keto–enol tautomerzation is thermodynamically easy to occur in the polar solvents and not in the apolar solvents. Therefore, the racemization was effectively prohibited in the apolar solvents. Furthermore, the secondary structure of the polymer strands may also be a factor affecting racemization. The formation of an enol structure may be restricted in the α-helical structure because of the

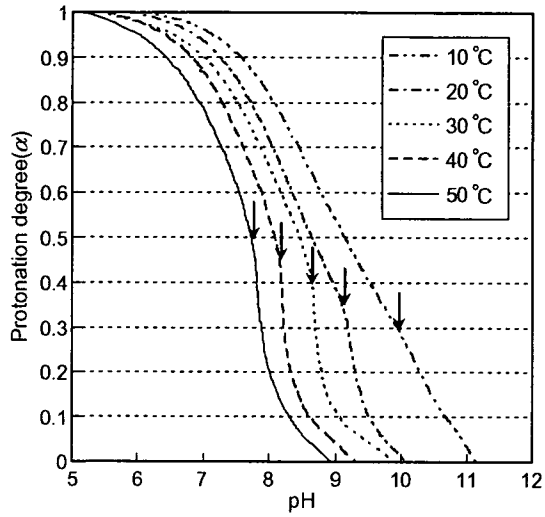

Fig. 7. Protonation degree (α) as a function of pH (α/pH curve) for PAsp(DIP) prepared in DMF. Each arrow in the figure indicates the pH at which the transmittance of the polymer solution decreased to 95%.

intramolecular hydrogen bond. However, further analyses may be needed to clearly explain the reaction scheme.

3.5. Solution properties of PAsp(DIP)

The analysis of the aqueous solution property of PAsp(DIP) synthesized in DMF was performed by the potentiometric titration and transmittance measurement to obtain α–pH curves at various temperatures (Fig. 7). The transmittance sharply decreased at a specific pH for all of the measuring temperatures, suggesting that the polymer became hydrophobic with the deprotonation to precipitate out of the solution.

The apparent pK_a ($pK_{a,app}$) values defined as a pH of $\alpha = 0.5$ increased with the decrease of the temperature from $pK_{a,app} = 7.7$ at 50 °C to $pK_{a,app} = 9.3$ at 10 °C. These results indicate that at a higher temperature, PAsp(DIP) is more liable to release proton because it is energetically preferable for the amphiphilic polycations to release highly condensed protons on the polymer strand to form the collapsed globule. However, stabilization due to the hydrophobic hydration was promoted at a lower temperature to maintain the solubility of PAsp(DIP) even at the higher range of pH. Eventually, PAsp(DIP) will be feasible to use as a novel smart materials with dual sensitivity i.e., sensitivity to both pH and temperature.

4. Conclusion

It was revealed that the aminolysis of PBLA, which proceeds involving a succinimide intermediate, was useful for quantitatively introducing the functional group into the side chain of PBLA. Moreover, racemization was effectively suppressed through the aminolysis in CH_2Cl_2 to give polyaspartamide with an appreciably high optical purity of 95%. This optical purity will apparently be a great advantage in its application as biomaterials. The cationic PAsp(DIP) synthesized by this method showed the dual sensitivity to pH and temperature, and thus may have a potential utility as novel smart biomaterials. In conclusion, this method of aminolysis is a simple and efficient way of constructing a polyaspartamide library from PBLA as a single platform polymer, and can be applied for screening the various utilities of structurally well-defined polyaspartamide derivatives as functionality materials.

Acknowledgements

The authors wish to express their gratitude to Prof. T. Tsuruta, Professor Emeritus, The University of Tokyo, for his valuable discussions and critical comments on this research. This work was financially supported by the Core Research for Evolutional Science and Technology (CREST) from the Japan Science and Technology Agency (JST).

References

[1] S. Jean-Claude, B. Jean-Claude, React. Polym. 12 (1990) 3.
[2] S. Jean-Claude, B. Jean-Claude, React. Polym. 12 (1990) 133.
[3] S. Jean-Claude, B. Jean-Claude, React. Polym. 13 (1990) 1.
[4] R. Arshdy, Adv. Polym. Sci. 111 (1994) 1.
[5] H. Mao, C. Li, Y. Zhang, S. Furyk, P.S. Cremer, D.E. Bergbreiter, Macromolecules 37 (2004) 1031.
[6] A. Godwin, M. Hartenstein, A.H.E. Müller, S. Brocchini, Angew. Chem. Int. Ed. 40 (2001) 594.
[7] W. Wu, B. Jin, G. Krippner, K. Watson, Bioorg. Med. Chem. Lett. 10 (2000) 341.
[8] L.E. Strong, L.L. Kiessling, J. Am. Chem. Soc. 121 (1999) 6193.
[9] A. Carrillo, K. Gujraty, P. Rai, R. Kane, Nanotechnology 16 (2005) S416.
[10] P. Strohriegl, Makromol. Chem. 194 (1993) 363.
[11] Y.S. Yang, G.R. Qi, J.W. Qian, S.L. Yang, J. Appl. Polym. Sci. 68 (1998) 665.
[12] Y.X. Liu, Z.J. Du, Y. Li, C. Zhang, C.J. Li, X.P. Yang, H.Q. Li, J. Appl. Polym. Sci. 44 (2006) 6880.
[13] R. Luxenhofer, R. Jordan, Macromolecules 39 (2006) 3509.

[14] B. Parrish, R.B. Breitenkamp, T. Emrick, J. Am. Chem. Soc. 127 (2005) 7404.
[15] T.J. Deming, Adv. Drug. Deliv. Rev. 54 (2002) 1145.
[16] S. Brocchini, Adv. Drug. Deliv. Rev. 53 (2001) 123.
[17] M. Ali, S. Brocchini, Adv. Drug. Deliv. Rev. 58 (2006) 1671.
[18] A. Lavasanifar, J. Samuel, G.S. Kwon, Adv. Drug. Deliv. Rev. 54 (2007) 169.
[19] G. Pratesi, G. Savi, G. Pezzoni, O. Bellini, S. Penco, S. Tinelli, F. Zunino, Brit. J. Cancer 52 (1985) 841.
[20] H.J.-P. Ryser, W.-C. Shen, Proc. Natl. Acad. Sci. USA 75 (1978) 3867.
[21] G.Y. Wu, C.H. Wu, J. Biol. Chem. 262 (1987) 4429.
[22] N. Lupu-Lotan, A. Yaron, A. Berger, M. Sela, Biopolymers 3 (1965) 625.
[23] A.D. Marre, H. Soyez, E. Schacht, J. Pytela, Polymer 35 (1994) 2443.
[24] M.G. Meirim, E.W. Neuse, F. Parisi, Angew. Makromol. Chem. 175 (1990) 141.
[25] E.W. Neuse, A.G. Perlwitz, S. Schmitt, Angew. Makromol. Chem. 181 (1990) 153.
[26] E.W. Neuse, A.G. Perlwitz, S. Schmitt, Angew. Makromol. Chem. 192 (1991) 35.
[27] E.W. Neuse, B.B. Patel, C.W.N. Mbonyana, J. Inorg. Organomet. Polym. 1 (1991) 147.
[28] J.C. Swarts, E.W. Neuse, G.J. Lamprecht, J. Inorg. Organomet. Polym. 4 (1994) 143.
[29] R.W. Niven, F. Rypacek, P.R. Byron, Pharm. Res. 7 (1990) 990.
[30] M. Schwamborn, Polym. Degrad. Stab. 59 (1998) 39.
[31] K.C. Low, A.P. Wheeler, L.P. Koskan, Adv. Chem. Ser. 248 (1996) 99.
[32] T. Nakato, M. Yoshitake, K. Matsubara, M. Tomida, T. Kakuchi, Macromolecules 31 (1998) 2107.
[33] S.K. Wolk, G. Swift, H.-P. Yi, K.M. Yocom, R.L. Smith, E.S. Simon, Macromolecules 27 (1994) 7613.
[34] K. Itaka, N. Kanayama, N. Nishiyama, W.-D. Jang, Y. Yamasaki, K. Nakamura, H. Kawaguchi, K. Kataoka, J. Am. Chem. Soc. 126 (2004) 13612.
[35] S. Fukushima, K. Miyata, N. Nishiyama, N. Kanayama, Y. Yamasaki, K. Kataoka, J. Am. Chem. Soc. 127 (2005) 2810.
[36] Y. Bae, W.-D. Jang, N. Nishiyama, S. Fukushima, K. Kataoka, Mol. Biosyst. 1 (2005) 242.
[37] A. Koide, A. Kishimura, K. Osada, W.-D. Jang, Y. Yamasaki, K. Kataoka, J. Am. Chem. Soc. 128 (2006) 5988.
[38] N. Kanayama, S. Fukushima, N. Nishiyama, K. Itaka, W.-D. Jang, K. Miyata, Y. Yamasaki, U.-I. Chung, K. Kataoka, Chem. Med. Chem. 1 (2006) 439.
[39] Arnida, N. Nishiyama, N. Kanayama, W.-D. Jang, Y. Yamasaki, K. Kataoka, J. Control. Release 115 (2006) 208.
[40] H.G. Schild, Prog. Polym. Sci. 17 (1992) 163.
[41] D.D. Perrin, W.L.F. Armarego, D.R. Perrin, Purification of Laboratory Chemicals, Pergamon, Oxford, 1980.
[42] K. Nokihara, J. Gerhardt, Chirarity 13 (2001) 431.
[43] P. Dubin, F.E. Karasz, Biopolymer 11 (1972) 1745.
[44] R.H. Karlson, K.S. Norland, G.D. Fasman, E.R. Blout, J. Am. Chem. Soc. 82 (1960) 2268.
[45] E.R. Blout, Biopolymers Symp. 1 (1964) 397.
[46] A.J. Adler, G.D. Fasman, E.R. Blout, J. Am. Chem. Soc. 85 (1963) 90.
[47] C.G. Swain, J.F. Brown, J. Am. Chem. Soc. 74 (1952) 2538.
[48] J.L. Radkiewicz, H. Zipse, S. Clarke, K.N. Houk, J. Am. Chem. Soc. 118 (1996) 9148.
[49] G.G. Smith, G.V. Reddy, J. Org. Chem. 54 (1989) 4529.
[50] T. Takata, T. Shimo-Oka, K. Miki, N. Fujii, Biochem. Biophys. Res. Commun. 334 (2005) 1022.
[51] N. Fujii, K. Harada, Y. Momose, N. Ishii, M. Akaboshi, Biochem. Biophys. Res. Commun. 263 (1999) 322.
[52] N. Fujii, L.J. Takemoto, Y. Momose, S. Matsumoto, K. Hiroki, M. Akaboshi, Biochem. Biophys. Res. Commun. 265 (1999) 746.
[53] A.C.T. Van Duin, M.J. Collins, Org. Geochem. 29 (1998) 1227.
[54] T. Nakato, A. Kusuno, T. Kakuchi, J. Polym. Sci. Part A: Polym. Chem. 38 (2000) 117.

DOI: 10.1002/cmdc.200700093

pH-Responsive Multi-PEGylated Dual Cationic Nanoparticles Enable Charge Modulations for Safe Gene Delivery

May P. Xiong,[a] Younsoo Bae,[b] Shigeto Fukushima,[c] M. Laird Forrest,[a] Nobuhiro Nishiyama,[b] Kazunori Kataoka,*[b, c] and Glen S. Kwon*[a]

In gene therapy, the cytotoxicity of many polycations is undesirable and has been attributed to nonspecific membrane destabilizing effects and intracellular polyplex-mediated toxicity. To help prolong the pharmacokinetic profile of nonviral vehicles for gene delivery, the cationic surface charge of current systems is typically shielded through the conjugation of polyethylene glycol (PEG) chains to the particle surface. However, the design of an intelligent polycation with environment-sensing charge modulations is essential to minimize cytotoxicity and enhance gene expression. We have designed a novel di-cationic block copolymer, poly(aspartate-hydrazide)-block-poly(L-lysine), capable of pH-mediated endosomal membrane disruption based on charge interactions, which has negligible toxicity elsewhere to the cell. The poly(L-lysine) segment, with a high pK_a value of ~9.4, preferentially forms a poly-ion complex with the negative phosphate groups of pDNA, whereas the pH-responsive poly(aspartate-hydrazide) segment, with the comparatively lower pK_a ~5.0, is characterized by a substantial fraction of unprotonated amino groups at physiological pH. As a consequence, complexation between such a polymer and pDNA leads to the formation of a two-layered nanoparticle. In particular, the nanoparticle possesses an unprotonated pH-responsive segment to serve as both a scaffold for acid-labile linkages of various moieties such as aldehyde-PEG and to transition from neutral to charged for disrupting endosomal membranes, and safely enhancing gene expression. Our system supports an endosomal escape mechanism based on charge interactions rather than the proton-sponge effect, and may be an important step towards engineering new classes of intelligent nonviral vectors.

Introduction

Intelligent biomaterials that can emulate natural viruses by adapting to their environment with minimal toxicity to the cell are highly desired for gene therapy. These synthetic vehicles are often internalized in many different cell lines through receptor-mediated endocytosis into clathrin-coated vesicles that fuse to form early endosomes (pH 7.4–6), which become late endosomes (pH 6.0–5.5), and eventually lysosomes (pH 5.0).[1–3] Research to date has primarily emphasized gene delivery carriers equipped with endosomal buffering, also known as the proton sponge effect (PSE),[4] to escape acidic endolysosomes for mediating gene expression.[5,6] However, natural viruses are not equipped with endosomal buffering properties. Instead, they frequently exploit the decrease in pH to expose fusogenic domains that can disrupt the endosomal or lysosomal membrane, resulting in release of the virus into the cytoplasm. Similarly, endosomal membrane disruptions with charged surfaces may also play an important role in helping particles escape from endosomes.[7,8] Despite their positive attributes, many common polycations are cytotoxic due to nonspecific membrane destabilizing effects and intracellular polyplex-mediated toxicity.[9–12] From these observations, we have postulated that the appreciable effect of charge interaction on endosomal escape might be observed even in the absence of the PSE by designing a pH-responsive polycation with dual functional pK_a values (high and low) to emulate the escape mechanism used by natural viruses.

[a] Dr. M. P. Xiong, Dr. M. L. Forrest, Prof. G. S. Kwon
Division of Pharmaceutical Sciences
School of Pharmacy, University of Wisconsin
777 Highland Avenue, Madison, WI 53705-2222 (USA)
Fax: (+1) 608-262-5345
E-mail: gskwon@pharmacy.wisc.edu

[b] Dr. Y. Bae, Dr. N. Nishiyama, Prof. K. Kataoka
Center for Disease Biology and Integrative Medicine
Graduate School of Medicine, The University of Tokyo
7-3-1 Hongo, Bunkyo-ku, Tokyo 113-0033 (Japan)
and
Center for NanoBio Integration, The University of Tokyo
7-3-1 Hongo, Bunkyo-ku, Tokyo 113-8656 (Japan)
Fax: (+81)3-5841-7139
E-mail: kataoka@bmw.t.u-tokyo.ac.jp

[c] Dr. S. Fukushima, Prof. K. Kataoka
Department of Materials Engineering
Graduate School of Engineering, The University of Tokyo
7-3-1 Hongo, Bunkyo-ku, Tokyo 113-8656 (Japan)

Supporting information for this article is available on the WWW under http://www.chemmedchem.org or from the author.

Results and Discussion

Chemical synthesis

Figure 1 shows the chemical structure of the dual-cationic block copolymer, poly(aspartate-hydrazide)-*block*-poly(L-lysine) (abbreviated BC), based on functional pK_a differences between respective cationic blocks. The poly(L-Lys) (PLL) segment, with a high pK_a value of ~9.4, preferentially forms a poly-ion complex (PIC) with the negative phosphate groups of pDNA, whereas the pH-responsive poly(Asp-Hyd) segment, with a comparatively lower pK_a value of ~5.0, is characterized by a substantial fraction of unprotonated amino groups at physiological pH (Figure 1a). Some of these Asp-Hyd residues are coupled to aldehyde-PEG chains (ALD-PEG) through acid-labile hydrazone linkages to impart favorable stealth properties to the PIC (Figure 1b). As a consequence, the complexation between such a polymer and pDNA may lead to the formation of a two-layered particle possessing an unprotonated pH-responsive poly(Asp-Hyd) segment that functions as both a scaffold for acid-labile linkages of various moieties, and that has the ability to undergo a transition from neutral to charged for disrupting endosomal membranes, as illustrated in Figure 2. Therefore, the PIC described herein is formed from associations of such block copolymer chains: a) a pDNA condensing core made of PLL chains (known for not contributing to the PSE), and b) a shell composed of segments with repeating Asp-Hyd residues.

The backbone of the block copolymer is derived from poly(β-benzyl-L-aspartate)-*block*-poly(L-lysine) (PBLA-*b*-PLL; see Supporting Information). PBLA was prepared by the ring-opening polymerization of β-benzyl-L-aspartate *N*-carboxyanhydride (BLA-NCA), initiated by the terminal $-NH_2$ group of butylamine to yield a polymer with narrow distribution and degree of polymerization (DP) of 36 (Figure 1S). The terminal amine on PBLA was used to initiate ring-opening polymerization of lysine(TFA) *N*-carboxyanhydride monomers (Lys-NCA) to yield PBLA-*b*-PLL(TFA) with DP = 53, in accordance with previous work in which a PLL length of ~50 was determined optimal for gene expression (Figure 2S).[5,13] Next, hydrazide groups were conjugated with a substitution efficiency near 100 mol% on PBLA, using a procedure reported by Bae et al.,[14,15] to give poly(Asp-Hyd)-*b*-PLL(TFA) (TFA = trifluoroacetyl). When deprotected, this polymer yields BC. Finally, ALD-PEG (M_W = 7000 g mol^{-1}) was synthesized following procedures reported by Nagasaki et al.[16] and characterized with ^{1}H NMR ($CDCl_3$; determined 91% acetal conversion into aldehyde groups) and gel permeation chromatography (GPC) (TSK-gel G3000PWXL and TSK-gel G4000PWXL; 10 mM LiCl in *N,N*-dimethylformamide (DMF); 0.8 mL min^{-1}; polydispersity index (PDI): 1.03). The final PEGylated block copolymers [poly(Asp-Hyd-PEG)-*b*-PLL] had either five ALD-PEG chains conjugated to each poly(Asp-Hyd) block to form the acid-labile hydrazone linkage (pH-PBC), or six COOH-PEG chains conjugated covalently by amide linkages to hydrazide groups to generate the non-hydrolysable control (cov-PBC), as shown in Figures 3S and 4S. There are substantial unconjugated hydrazide groups that remain on each block copolymer chain.

Physical characterization

The protonation profile of BC reveals that hydrazide groups do not significantly buffer in the critical range known to be essential for PSE-mediated escape of endosomes (pH 5.0–6.0), similar

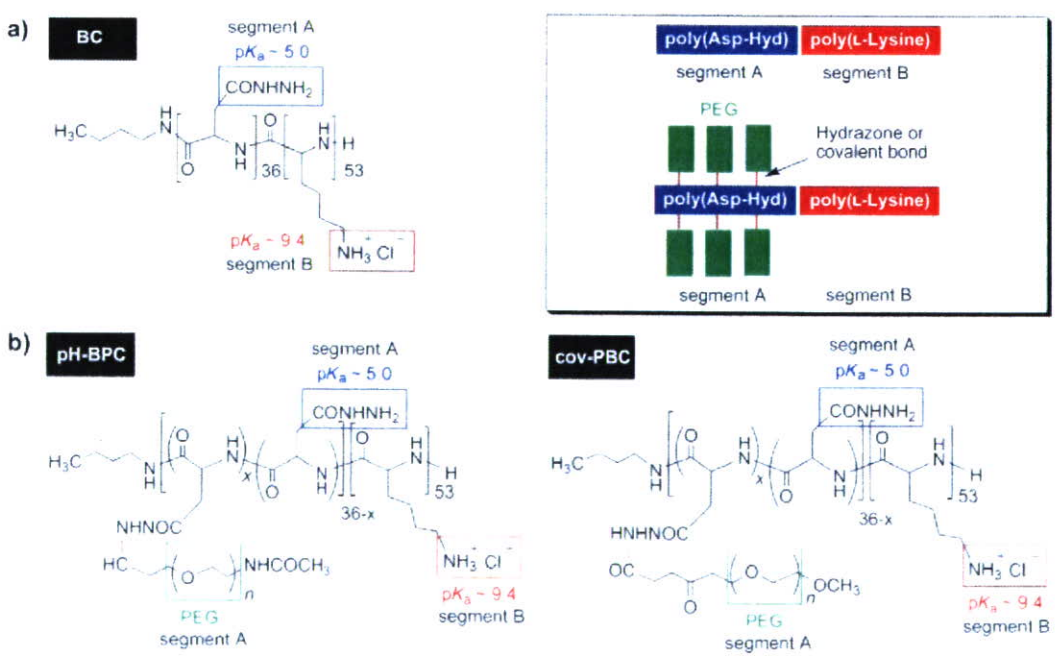

Figure 1. Structure of the block copolymers: a) poly(aspartate-hydrazide)-*block*-poly(L-lysine) (BC); b) pH-sensitive poly(aspartate-hydrazide-PEG)-*block*-poly(L-lysine) (pH-PBC), and covalent poly(aspartate-hydrazide-PEG)-*block*-poly(L-lysine) (cov-PBC). (See Supporting Information for synthesis.)

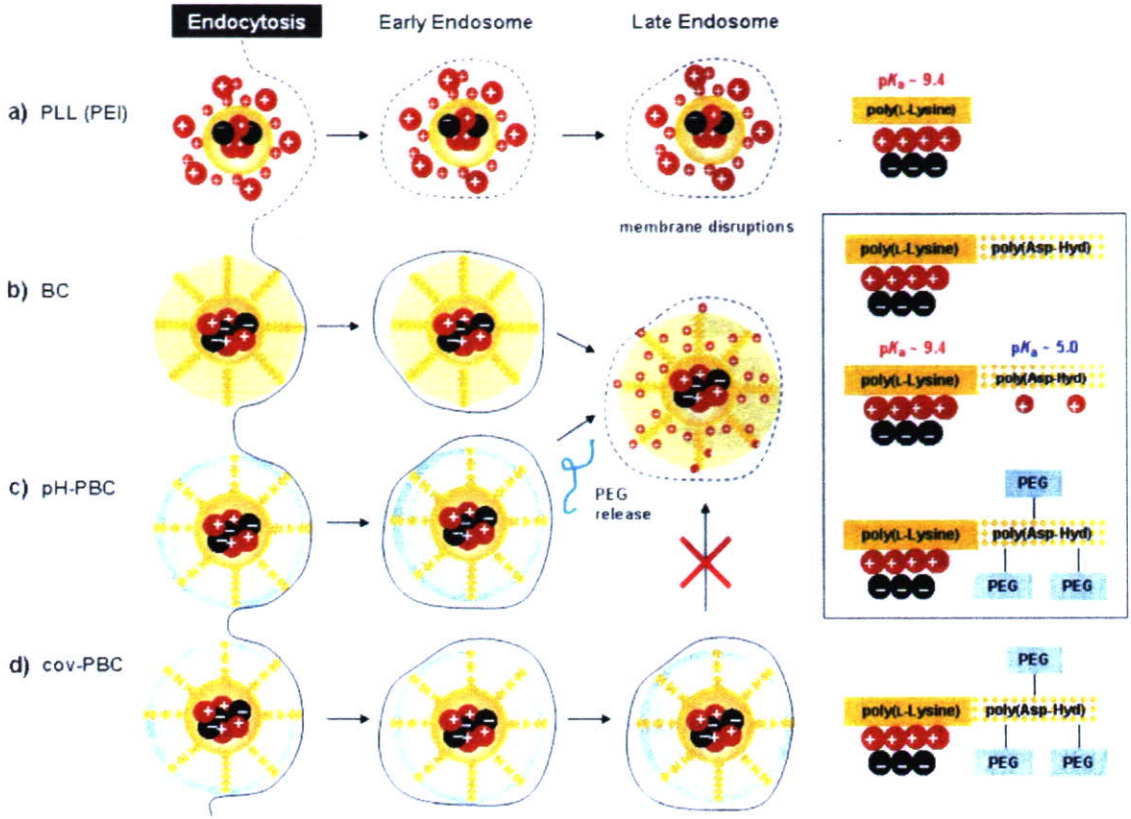

Figure 2. a) Cationic polyplexes formed with PLL (or PEI) are cytotoxic to cells. In contrast, neutral shielded particles [parts b), c), and d)] cause minimal membrane damage during endocytosis: Following a decrease in pH, hydrazide amino groups protonate (b) and/or acid-labile PEG chains are released (c). This increases endosomal membrane disturbances with the resulting charged particle and enhances escape into the cytosol (pH 7.4), whereupon sensing the new pH, hydrazide amino groups deprotonate again, once more imparting neutral properties to the PIC and minimizing intracellular toxicity. d) cov-PBC particles cannot release PEG chains following a decrease in pH, and this may minimize particle interactions with the endosomal membrane.

to PLL (Figure 3), and furthermore do not contribute significantly to pGL3 condensation at physiological pH, because mostly PLL groups undergo electrostatic interactions with pDNA (Figure 4). This suggests that the PIC formed is composed of a PLL–DNA core with poly(Asp-Hyd) segments on the surface. The effect of pH on colloidal properties of the PIC was also investigated (Figure 5). At pH 7.4, PICs formed with BC have mostly unprotonated hydrazide groups exposed on the surface (~5.0 mV), and counterion screening causes particles to exhibit aggregation behavior (diameter ~440 nm). However, as hydrazide groups on PICs become protonated with decreasing pH, charged cationic surfaces are generated (~35 mV), overcoming van der Waals interactions and resulting in electrostatic repulsions between individual particles (~100 nm). For pH-PBC, the size and ζ profiles are more informative than the averages reported (Figure 5, insert). Although average $\zeta < 8$ mV and average diameter is < 100 nm over the range of pH, the system is represented by distinct multimodal populations, indi-

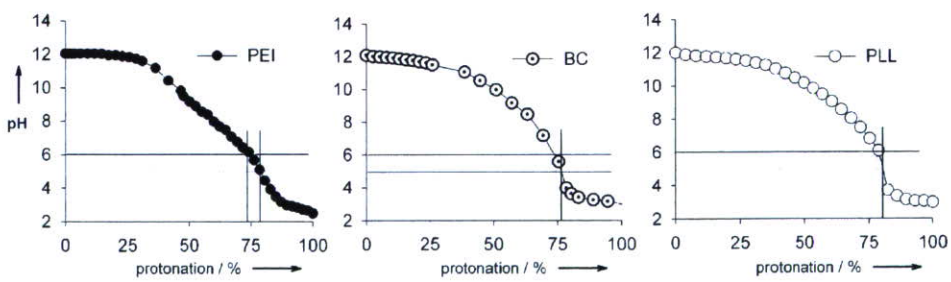

Figure 3. Protonation profiles comparing branched PEI, BC, and PLL. As expected, PEI can buffer over a relatively wide pH range. BC carries little buffering capacity, similar to PLL (note: error bars omitted to simplify profile). Table 1S summarizes the mol% of various amines on each polymer; only side chain terminal amines are considered. The data indicate that the presence of hydrazide groups on BC does not contribute significantly to endosomal buffering in the critical range of pH 5.0–6.0 essential to the PSE.

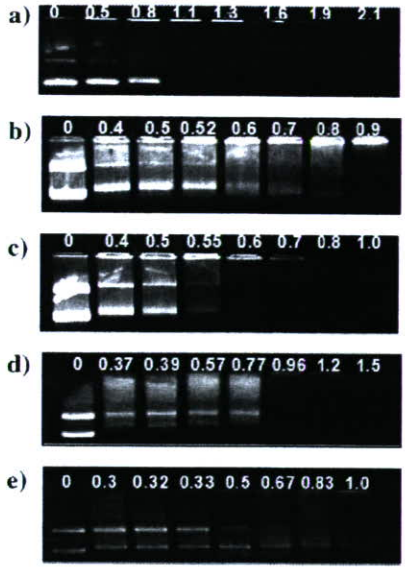

Figure 4. Isoelectric points (pI) of the polymer in complex with 1 μg pGL3; values indicate equivalent N/P ratios: a) PEI (25 000 g mol^{-1}), pI (*w*/*w*) = 0.20 μg, N/P = 1.1; b) BC (poly(Asp-Hyd)$_{36}$-PLL$_{49}$) (11 000 g mol^{-1}), pI (*w*/*w*) = 0.65 μg, N/P = 0.9; c) PLL$_{44}$ (9200 g mol^{-1}), pI = 0.40 μg, N/P = 0.7; d) pH-PBC (five PEG chains per BC, 46 000 g mol^{-1}), pI = 2.5 μg, N/P = 0.96; e) cov-PBC (six PEG chains per BC, 53 000 g mol^{-1}), pI = 4 μg, N/P = 1.0. Electrostatic interactions occur mostly between lysine groups and pGL3, as BC and PBC polymers have similar N/P ratios of ~1.

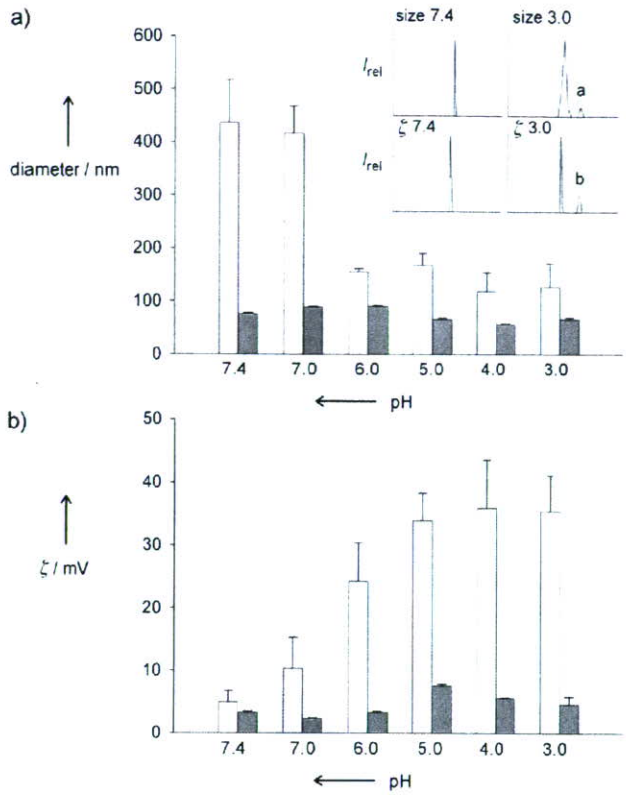

Figure 5. a) Size and b) ζ profiles for BC (white) and pH-PBC (gray) at the indicated pH values. Particles were formed at N/P = 20 (to concur with the transfection experiments) with 2 μg pGL3 in water, incubated for at least 30 min, and diluted with low-ionic-strength buffers of appropriate pH before size measurement. The same sample was then injected into the instrument to obtain ζ potentials. At pH 7.4, BC particles are ~440 nm with ζ potentials of ~5 mV. At pH 3.0, BC particles are ~100 nm with ζ potentials of ~35 mV. For pH-PBC, the particles are ~80 nm in diameter with a ζ value of ~3 mV at pH 7.4. At pH 3.0, the average size is ~70 nm and ζ ~5 mV. However, pH-PBC profiles under acidic conditions (insert) point to particle instability as PEG is released. Large aggregates (peak a) with higher ζ values (peak b) appear (multimodal populations were observed for all acidic pH values). In contrast, cov-PBC had single population profiles (data not shown). (Note: the values reported were calculated by averaging the sums of peak intensities multiplied by magnitudes.)

cative of reversible PEG release. This is in sharp contrast to the single population observed with cov-PBC under acidic conditions (data not shown). pH-Release studies confirm that, in a closed system, the hydrazone linkage is reversible and exhibits equilibrium behavior at various pH values over prolonged incubation (Figure 6).

Biological characterization

In addition, subsequent lactate dehydrogenase (LDH) release studies show that our dual-cationic polymer does not cause membrane toxicity when complexed with pDNA. At physiological pH, free PEI, PLL, and BC polymer chains have cationic properties that cause high levels of membrane toxicity to cells, relative to PEG-shielded polymers (Figure 7a,c). However, if BC (20 μg mL^{-1}) is complexed with pGL3, the presence of many unprotonated hydrazides on the surface of the PIC causes negligible membrane toxicity (Figure 7b). As BC concentration is increased in the presence of pGL3 (40 μg mL^{-1}), LDH release also increases, but that is most likely due to the presence of excess free polymers in solution with respect to pDNA concentration (Figure 7d). Our results imply that freely accessible charged polymers cause membrane-associated toxicity, but that membrane damage is minimized when the cationic PLL block is concealed within the PIC core.

We next compared the metabolic activity of our polymers both in free form and in complex with pGL3 to investigate the potential intracellular toxicity often associated with cationic polyplex-mediated uptake.[12] The free polymers (PEI and BC) with accessible cationic components caused greater metabolic toxicity to the cell following internalization (Figure 8a). PEG-shielded polymers exhibited low metabolic toxicity. On the other hand, PICs with concealed cationic PLL cores (BC, pH-PBC, and cov-PBC) gave little evidence of metabolic toxicity to the cell, in contrast to PEI-formulated particles (Figure 8b). These results correspond well with the LDH assay data.

Finally, we looked at the transfection efficiency of these polymers in five very different cell lines and found that pH-PBC and BC (both nontoxic) consistently resulted in higher gene expression relative to cov-PBC (Figure 9) and PLL (data not shown). Note that the trend in transfection between the polymers and across different cell lines is not consistent. This might be a result of the fact that in the absence of targeting ligands, various cell lines use different modes of particle internalization (such as clathrin and/or caveolae-mediated processes) that can ultimately affect uptake pathways and particle fate within the cell.[17–19] Importantly, however, there is a consistent

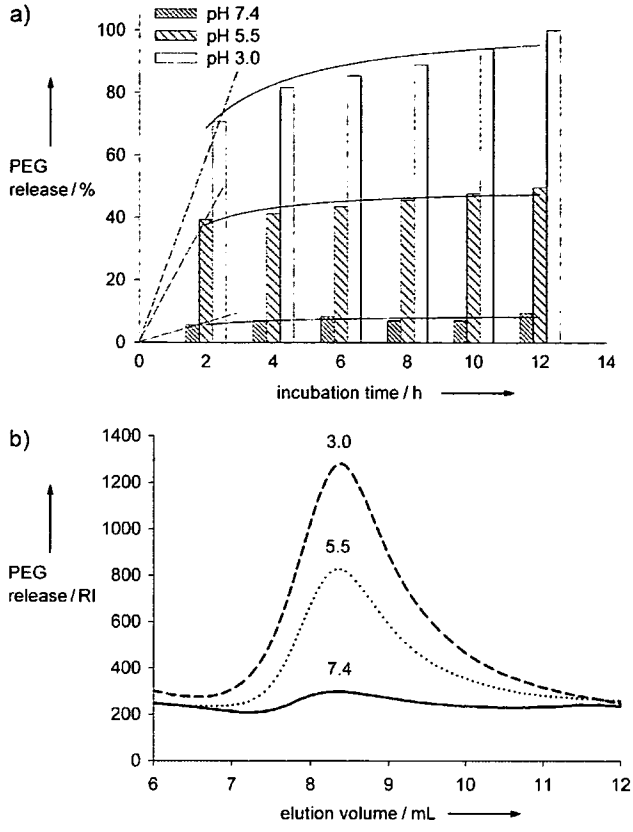

Figure 6. PEG release monitored by GPC: pH-PBC was injected into an OHpak SB-806M GPC column (injection volume: 20 μL; polymer: 2 mg mL^{-1}; of HEPES eluent: 10 mM, pH 7.4, 0.75 mL min^{-1}, 30 °C; Shodex, Kawasaki, Japan), and PEG release was detected by refractive index (RI) for 12 h. a) PEG falls off upon incubation at pH < 7.0, but the hydrazone bond is relatively stable at pH 7.4, with less than 10% PEG released over 12 h. The reversible nature of the hydrazone bond leads to an equilibrium state in the release profiles at different pH's. b) Sample curves at $t = 2$ h are shown with pH values indicated.

enhancement in gene expression for BC and pH-PBC compared with cov-PBC in the cell lines investigated. This demonstrates that a dynamic approach for release of PEG from BC is beneficial to increase endosomal membrane disruptions with charged particles, as the presence of PEG can minimize membrane interactions in the absence of charge.[20]

It is of significant interest that our dual-cationic PICs suggest an endosomal escape mechanism for polyplexes which might be attributed to disruptions based on cationic-mediated cellular membrane interactions rather than through the PSE. In other words, selectively controlling interactions between polyplexes and the cell membrane is a new and facile approach for the design of effective and high-performance nonviral gene vectors. This results in nonviral vectors that are both safe to the cell while retaining high transfection efficiencies. Indeed, unlike PEI, which induces effective transfection activity but also causes high levels of nonspecific membrane-associated toxicity (Figure 2a), neutral shielded particles (BC, pH-PBC, and cov-PBC) result in cellular uptake with minimal toxicity to the membrane (Figure 2b–d). Upon sensing a decrease in pH, PEG chains are released from pH-PBC PICs, and the remaining BC particle acquires favorable cationic properties for disrupting endosomal membranes. After the particles escape into the cytosol (pH 7.4), hydrazide groups start to deprotonate upon sensing the new pH, imparting neutral properties to the PIC again. This is very similar to how natural viruses respond to their environment by exposing a fusogenic domain at low pH and concealing it at higher pH, and may explain the low metabolic toxicity of PICs in the cell.

Conclusions

In summary, we have designed an intelligent polycation with dual functional pK_a values capable of safely emulating the escape mechanism used by natural viruses. This novel dual-cationic block copolymer, poly(Asp-Hyd)-*b*-PLL, is pH-mediated to disrupt endosomal membranes based largely on charge interactions, and is therefore minimally toxic to the cell elsewhere. This is a mechanism separate from the traditional PSE followed by osmotic rupture of the vesicle. Furthermore, the significant presence of unconjugated hydrazides on the block copolymer can serve as a scaffold for easily incorporating many additional pH-sensitive functionalities, in addition to ALD-PEG, to the PIC to boost gene expression further. Examples of this include PEG-shielded fusogenic peptides for endosomal escape, nuclear localization signals (NLS), dynein-binding moieties, and additional masked targeting peptides for nuclear localization.[21,22] Therefore, these findings offer a new platform for generating more effective and complex multifunctional biomaterials for increasing gene expression.

Experimental Section

General materials. Branched polyethylenimine (M_W = 25000 g mol^{-1}) and poly(L-lysine) hydrobromide (M_W = 9200 g mol^{-1}) were purchased from Sigma–Aldrich (Milwaukee, WI, USA). All materials were used without further purification. The pDNA encoding firefly luciferase (pGL3, 5.3 kb) was obtained from Promega (Madison, WI, USA), transformed into electrocompetent DH5α cells, propagated in LB broth (1 L) supplemented with ampicillin (100 μg mL^{-1}), and purified with a plasmid Maxiprep kit (BioRad, Hercules, CA, USA). All pDNA had purity levels of 1.8 or greater by UV/Vis (A_{260}/A_{280}). For cell culture work, Dulbecco's modified Eagle's medium (DMEM), RPMI 1640, phosphate buffered saline (PBS), fetal bovine serum (FBS), trypsin–EDTA (0.25% trypsin, 2.21 mM EDTA in Hank's balanced salt solution (HBSS)) and penicillin/streptomycin were purchased from Cellgro (Mediatech, Herndon, VA, USA).

Physical characterization. pH titration measurements for polymers were obtained with an Orion micro-combination pH/sodium electrode (Thermo Electron Corporation, Waltham, MA, USA; see Supporting Information for general procedures). Dynamic light scattering and ζ potential data were obtained with a nanoZS 90 or a Malvern 3000HS series zetasizer (Malvern Instruments, UK). Polymers were mixed to form PICs at N/P = 20 by addition of polymer to an equal volume of pGL3 in Milli-Q water. The sample was allowed to incubate at room temperature for at least 15 min before dilution with the appropriate buffer ranging from pH 7.4 to pH 3.0. Particle diameters and ζ potentials were measured following dilution at each pH value.

